Journal of Electronic Imaging 6(4), 467–478 (October 1997).

Adaptive feature enhancement for mammographic images with wavelet multiresolution analysis

Lulin Chen
University of Rochester
Department of Electrical Engineering
Rochester, New York 14627

Chang W. Chen
University of Missouri, Columbia
Department of Electrical Engineering
Columbia, Missouri 65211
E-mail: cchen@ece.missouri.edu

Kevin J. Parker
University of Rochester
Department of Electrical Engineering
Rochester, New York 14627

Abstract. *A novel and computationally efficient approach to an adaptive mammographic image feature enhancement using wavelet-based multiresolution analysis is presented. On wavelet decomposition applied to a given mammographic image, we integrate the information of the tree-structured zero crossings of wavelet coefficients and the information of the low-pass-filtered subimage to enhance the desired image features. A discrete wavelet transform with pyramidal structure is employed to speedup the computation for wavelet decomposition and reconstruction. The spatiofrequency localization property of the wavelet transform is exploited based on the spatial coherence of image and the principle of human psychovisual mechanism. Preliminary results show that the proposed approach is able to adaptively enhance local edge features, suppress noise, and improve global visualization of mammographic image features. This wavelet-based multiresolution analysis is therefore promising for computerized mass screening of mammograms.*
 [S1017-9909(97)00704-6]

1 Introduction

Early diagnosis of cancers is an essential and important step to reduce mortality from these diseases. For breast cancer, one of leading causes of cancer deaths among women, screen/film mammography is currently considered to be the best and the most practical radiological technique for early detection of small breast tumors.[1] The presence of microcalcification in mammograms is of great clinical importance for early radiological diagnosis. Radiologists use this type of signature to discriminate normal tissues from abnormal or cancerous ones. However, even well-trained radiologists misdiagnose 10 to 20% of mammograms.[2,3]

For a realistic mass screening of mammograms, computer-assisted diagnosis (CAD) is desired for a fast and operator-independent analysis of massive volumes of mammographic images. It has also been shown that CAD has the potential to reduce the misdiagnosis rate.[4] In general, three operations are required in CAD, namely, feature enhancement, noise suppression, and feature extraction. There are many attempts on CAD with digital mammography.[5–11] However, adaptive and robust algorithms are still needed to integrate these operations.

The wavelet transform has recently been applied to digital mammography for feature enhancement and extraction with promising potential.[12–16] The framework of current wavelet-based mammographic image feature enhancement and extraction follows a general pattern: image decomposition with the forward wavelet transform, linear or nonlinear processing over the wavelet coefficients, and image reconstruction with the inverse wavelet transform. In general, edge-related information[17–20] is used to guide the linear or nonlinear processing. These edges are often obtained from the multiscale edge detectors by smoothing the signal at various scales and detecting sharp variation points from the extrema of their first-order derivatives and the zero crossings of their second-order derivatives. Several researchers[12,14,15] have presented some interesting and encouraging results using wavelet transform in digital mammography. Laine *et al.*[12] used a 2-D dyadic wavelet transform and performed edge-related analysis on the wavelet coefficients for feature enhancement. Strickland and Hahn[15] applied the matched filter concepts to combine with the wavelet transform for the detection of microcalcifications. Both approaches seek to process the high-pass-filtered subimages to extract information of maximum coefficients for enhancement purpose. These processings are executed with

Paper IST-07 received Jan. 13, 1997; revised manuscript received May 22, 1997; accepted for publication May 29, 1997.
1017-9909/97/$10.00 © 1997 SPIE and IS&T.

full resolution of images at each level without downsampling. In general, the information at different levels is processed separately without exploiting the information across different levels as well as the information in low-pass-filtered subimage.

It is well known that wavelet-based image analysis has two distinct characteristics: multiresolution and spatiofrequency localization.[21,22] To take full advantage of the wavelet-based analysis, these two characteristics must be optimally integrated with the desired image processing tasks. Multiresolution refers to the characteristics of the image analysis such that a feature can appear at different levels of subimages. In the case of mammographic image analysis, multiresolution analysis enables the feature enhancement and extraction to combine information from several channels at different resolution levels to obtain a robust estimate with efficient processing. With spatiofrequency localization, an abrupt change in image intensity can appear in high-pass-filtered subimages with accurate spatial location. This is quite different from the traditional Fourier analysis since the spatial information is lost after Fourier transform, and the windowed or short-time Fourier transform, which has a fixed resolution in the spatial and frequency domains. In wavelet-filtered subimages, an isolated single-pixel intensity change can be considered as noise and should be suppressed, whereas abrupt intensity changes over extended regions can be considered as image irregularity or edge structures. These structures in mammographic images usually correspond to the microcalcification details that we would like to preserve.

In this paper, the framework of image analysis also follows the general pattern, that is, the enhancement is performed on the wavelet-filtered subimages. However, we integrate the information from several channels and different resolutions to maximize the potential of the multiresolution analysis and to exploit the human psychovisual mechanism. The cross-band integration is implemented by establishing a zero-crossing tree for the purpose of adaptive feature enhancement and noise suppression. Only these coefficients within the zero-crossing tree are considered related to mammographic features and are therefore enhanced. The low-pass-filtered subimage is used to guide the enhancement process according to human perceptual dependence on local intensity. Furthermore, instead of full resolution processing, a discrete wavelet transform with a pyramid structure is employed to speedup the computation for fast wavelet decomposition and reconstruction.

The concept of a zero-crossing tree is based on our observation that the filters for high-pass filtering with orthonormal or biorthogonal bases in discrete wavelet decompositions are of Laplacian-like property, i.e., they resemble the second-order-derivative operations. Therefore, zero crossings in wavelet coefficient space describe the edges of the original image depicted in a multiresolution space. Because of the spatial coherence of image, the same image feature structure, in general, would appear at different level of subimages. A similar feature structure in a parent subimage can be found in its corresponding location of the child subimage so that they constitute a parent-child location relation. Such parent-child location relation can be established as zero-crossing trees to represent evolution of the multiresolution edges. The neighborhood configuration has been introduced to obtain the adaptivity to the local intensity variation. By following the evolutions of these zero crossings, we will be able to enhance the desired image features while, at the same time, suppress the undesired noise.

To achieve the optimal visualization of the image structures, the enhancement of high-pass-filtered subimages based on a zero-crossing tree is then integrated with the enhancement of baseband subimage according to human psychovisual mechanism. Usually mammographic images have low contrast and sometimes low illumination. It is well known that human vision follows the famous Weber's law,[23] that is, brightness discrimination is poor at the extreme low or the extreme high levels of illumination, and it improves significantly as the brightness illumination increases from the extreme low or decreases from the extreme high. Therefore, the way we enhance a particular wavelet coefficient should also depend on the levels of illumination within its neighborhood. For low levels of illumination, a large amount of enhancement is desired, while for high levels of illumination, a moderate amount of enhancement may be sufficient. For this same reason, the baseband subimage may also be enhanced by increasing the overall level of illumination so that the brightness discrimination is maximized.

Images used in our experiments are obtained from the Mammography Image Analysis Research Database at the University of South Florida. These 40 images were made available by the Department of Radiology, University Hospital Nijmegen, the Netherlands. The preliminary results of enhancement on these images show that the technique is promising for computerized mass screening of mammograms since the proposed algorithm is able to adaptively enhance local edge features, suppress noise, and greatly improve global visualization of mammographic image features.

Section 2 briefly discusses the discrete wavelet transforms used in this research with a pyramid structure. Section 3 introduces the adaptive feature enhancement algorithm based on the proposed multiresolution analysis. We focus on the information integration aspect, which is the key to the success of the proposed approach. Section 4 presents the experimental results and Sec. 5 concludes this paper with a summary and some discussion of future research directions.

2 Wavelet Analysis

The wavelet transform of an image is computed by decomposing the given image using wavelet bases, and can be viewed as a decomposition using a set of frequency channels having a spatial orientation tuning. Unlike the traditional Fourier transform, which has no spatial resolution, and the windowed Fourier transform, which has a fixed resolution in the spatial and frequency domains, the resolution of wavelet transform varies with a scale factor. Therefore, wavelet representations lie between the spatial and frequency domains and provide a simple and efficient hierarchical framework for interpretation of image information from both the spatial and frequency domains. For mammographic images, generally, the structures such as microcalcifications that we want to recognize have different sizes and it is difficult to define in advance a moderate resolution

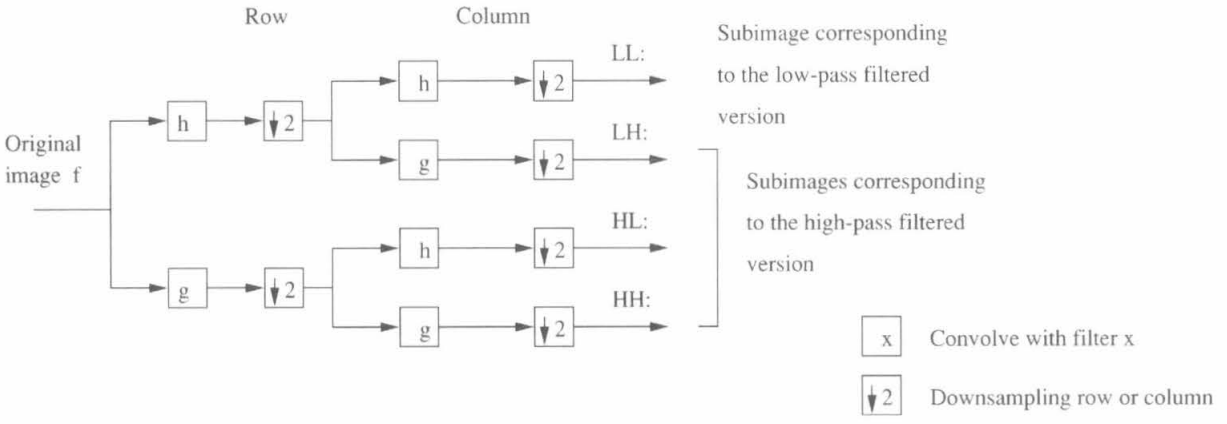

Fig. 1 Implementation of one-level 2-D discrete wavelet decomposition.

for analyzing image structures. With wavelet decomposition, we can exploit the image information efficiently and regroup the image information into a set of details appearing in subimages at different resolutions. At coarser resolutions, these details correspond to larger structures, while at finer resolutions these details correspond to smaller structures. The following is a brief review of some relations in discrete wavelet analysis.

For a discrete wavelet decomposition of a given 1-D signal f with a mother wavelet ψ and a scaling function ϕ and their dilated and translated versions, $\phi_{m,n}(x) = 2^{-m/2}\phi(2^{-m}x-n)$ and $\psi_{m,n}(x)=2^{-m/2}\psi(2^{-m}x-n)$, m and n are integers, we have the following relations[22]:

$$f=\sum c_{m,n}(f)\psi_{m,n},$$

$$c_{m,n}(f)=\langle\psi_{m,n},f\rangle=\sum_k g_{2n-k}a_{m-1,k}(f),$$

$$a_{m,n}(f)=\sum_k h_{2n-k}a_{m-1,k}(f), \tag{1}$$

where $g_l=(-1)^l h_{1-l}$ and $h_n=\sqrt{2}\int\phi(x-n)\phi(2-x)\,dx$. For these orthonormal wavelet bases, the exact reconstruction, at position l and level m, can be written as

$$a_{m-1,l}(f)=\sum_n [h_{2n-1}a_{m,n}(f)+g_{2n-1}c_{m,n}(f)]. \tag{2}$$

Equation (2) is a recursive relation that facilitates a fast computation algorithm. In the case of biorthogonal wavelet bases, the reconstruction becomes[24,25]

$$a_{m-1,l}(f)=\sum_n [\tilde{h}_{2n-l}a_{m,n}(f)+\tilde{g}_{2n-l}c_{m,n}(f)], \tag{3}$$

where the decomposition and reconstruction filters satisfy

$$\tilde{g}_n=(-1)^n h_{1-n}, \quad g_n=(-1)^n\tilde{h}_{1-n},$$

$$\sum_n h_n\tilde{h}_{n+2k}=\delta_{k,0}. \tag{4}$$

According to Mallat's paper,[22] 2-D wavelet representations for images can be similarly constructed with a separable 2-D wavelet transform, such as the scaling function $\phi(x)\phi(y)$ and the three 2-D wavelets $\psi(x)\phi(y)$, $\phi(x)\psi(y)$, and $\psi(x)\psi(y)$. The implementation of 2-D discrete wavelet decomposition (one level) is shown in Fig. 1. Each level consists of four subimages denoted as HL, LH, HH, and LL. HL exhibits the horizontal components (vertical edges), LH the vertical components (horizontal edges), and HH the components in both directions (corners). The LL corresponds the lowest frequencies and represents the local direct current (DC) components of the original image. Because of the bandwidth reduction after wavelet filtering, the resultant subimages can be downsampled to enable fast computation in the process of enhancement. Figure 2 shows the arrangement of subimages after discrete wavelet decomposition and downsampling on three levels.

The regularity and orthogonality of wavelet bases ensure the signal reconstruction with high quality. We choose short filters to enable fast computation. The shortest wavelet filters are those corresponding to the Haar basis, i.e., $h_0=h_1=\sqrt{2}$, $g_0=-g_1=\sqrt{2}$, and all other h_n, $g_n=0$. However, such filters result in less smoothness or regularity and lower efficiency in exploiting the spatial coherence of image structures in contrast to the spatial randomness of noise. In many image processing applications, smooth wavelet filters are desired to obtain better localization properties in both spatial and frequency domains. Therefore, a trade-off between the computational speed and the characterization of image features is usually needed for a specific application. In this research, we adopt the "Laplacian pyramid filters (5/7)" (Ref. 25) for the discrete wavelet transform because these filters are nearly orthonormal with moderate lengths.

3 Enhancement Algorithm

Once a mammographic image is decomposed with the given wavelet filter, the baseband subimage is essentially the replica of the original image with lower spatial resolution. However, the high-pass-filtered subimages with differ-

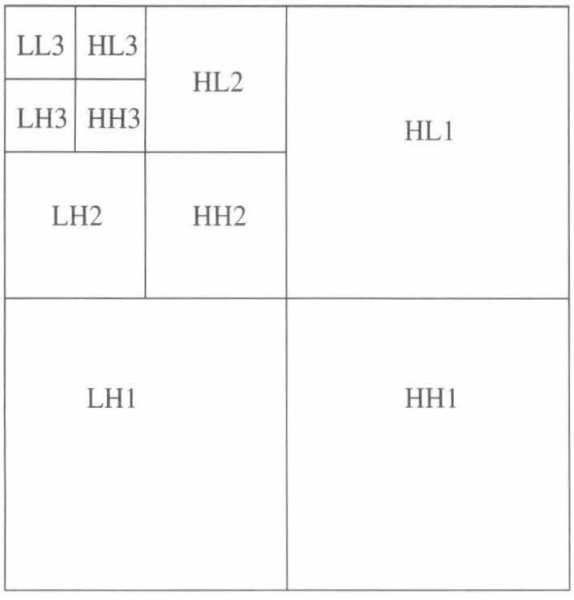

Fig. 2 Subimage arrangements of wavelet decomposition on three levels.

ent directional filtering and at different resolution levels would exhibit various edges corresponding to the filter directions and the resolution levels. A distinct feature of this approach different from existing ones is that we not only perform the enhancement on the individual high-pass-filtered subimages but also integrate the information from corresponding subimages at different levels using the parent-child relation and the information from baseband subimages according to human psychovisual mechanism.

In this section, we first summarize some characteristics of the wavelet-based multiresolution analysis. We then describe the proposed adaptive enhancement scheme designed to take full advantage of these characteristics to achieve optimal integration of information from different channels at different levels.

3.1 *Characteristics*

There are several distinct characteristics of the wavelet-filtered subimages that can be exploited in the design of an integrated adaptive enhancement algorithm. In this research, we explore three such characteristics: the baseband subimages, the zero crossings, and the parent-child location relations of the zero-crossing tree. Once these characteristics are carefully explored and the information from different channels are integrated, we expect to achieve better performance in image enhancement.

Unlike existing approaches in which the baseband subimage has not been used for feature enhancement, the proposed enhancement algorithm incorporates the information from baseband subimages to maximize the visual effect of enhancement. The incorporation of baseband subimage involves two types of operations: (1) global shift of baseband intensity value and (2) high-pass subimage enhancement weighted by the corresponding intensity value at baseband. Both operations are based on Weber's law of visual perception. An appropriate global shift of baseband intensity value ensures that the reconstructed images are bright enough to perceive the subtle brightness discriminations. Since the wavelet-based enhancement can be implemented by scaling the wavelet coefficients in high-pass subimages, the weighting of the baseband intensity value on the scaling implies that the algorithm is adaptive to the local illumination levels. This is important since according to human psychovisual mechanism, in particular Weber's law, brightness discrimination is poor at the extremely low levels of illumination, and it obeys the well-known proportional relation in midlevel illuminations. At the extremely high levels of illumination, a greater variation rate is required to sense brightness discriminations, in other words, human vision is not as sensitive to variation in this level. Therefore, an inverse weighting is suitable, so that, for the same edge strength, large scaling is required when the baseband intensity is low, and small scaling is adequate when the baseband intensity is high. It is evident that both operations are subject to the dynamic range limitation of the display devices.

In their classical paper, Marr and Hildreth[20] showed that the position of multiscale sharp variation points can be obtained from the zero crossings of the signal convolved with the Laplacian of a Gaussian. In the case of mammographic images, image features such as microcalcifications actually correspond to the intensity discontinuities. We noticed that the filters for LH, HL, and HH, high-pass filtering with orthonormal or biorthogonal bases, except Haar bases, in discrete wavelet decompositions are of Laplacian-like property, i.e., they resemble a second-order-derivative operation. The zero-crossing properties are still well preserved in these high-pass-filtered subimages even with downsampling in the pyramidal structure. Figure 3 shows examples of the zero crossings of a given image using "Spline variant filters (9/7)" and "Laplacian pyramid filters (5/7)" (Ref. 25). Notice that these zero crossings correspond to potential edges of the original image at multiresolution levels. Therefore, we assert that the zero crossings in the high-pass-filtered subimages are equivalent to the multiresolution edges of the original image. The multiresolution position information of the edges can be obtained from processing of the zero crossings of wavelet coefficients in the high-pass-filtered subimages.

Because of the spatial coherence of the image, image feature structures, in general, appear at different subimage levels. If we define the parent-child relation of a subimage as the relationship between subimages at a specific resolution level and the corresponding subimages at a finer resolution level, then an image feature structure in a parent subimage will have similar image features in its child subimage at corresponding locations. Such parent-child location relations are shown in Fig. 4. This parent-child spatial coherence relation can be very useful in zero-crossing analysis, since, for medical images, an isolated single-pixel intensity change in wavelet-filtered subimages can be considered as noise and should be suppressed, while abrupt intensity changes over a relatively large connected region can be considered as clinically important structures. For mammographic images, these coherent features usually correspond to the microcalcification details and should be preserved and preferably visually enhanced. On the other hand, this parent-child relation can also be used to suppress mammographic image noise because, as suggested by several researchers,[17,18,26] the sharp variation points of image

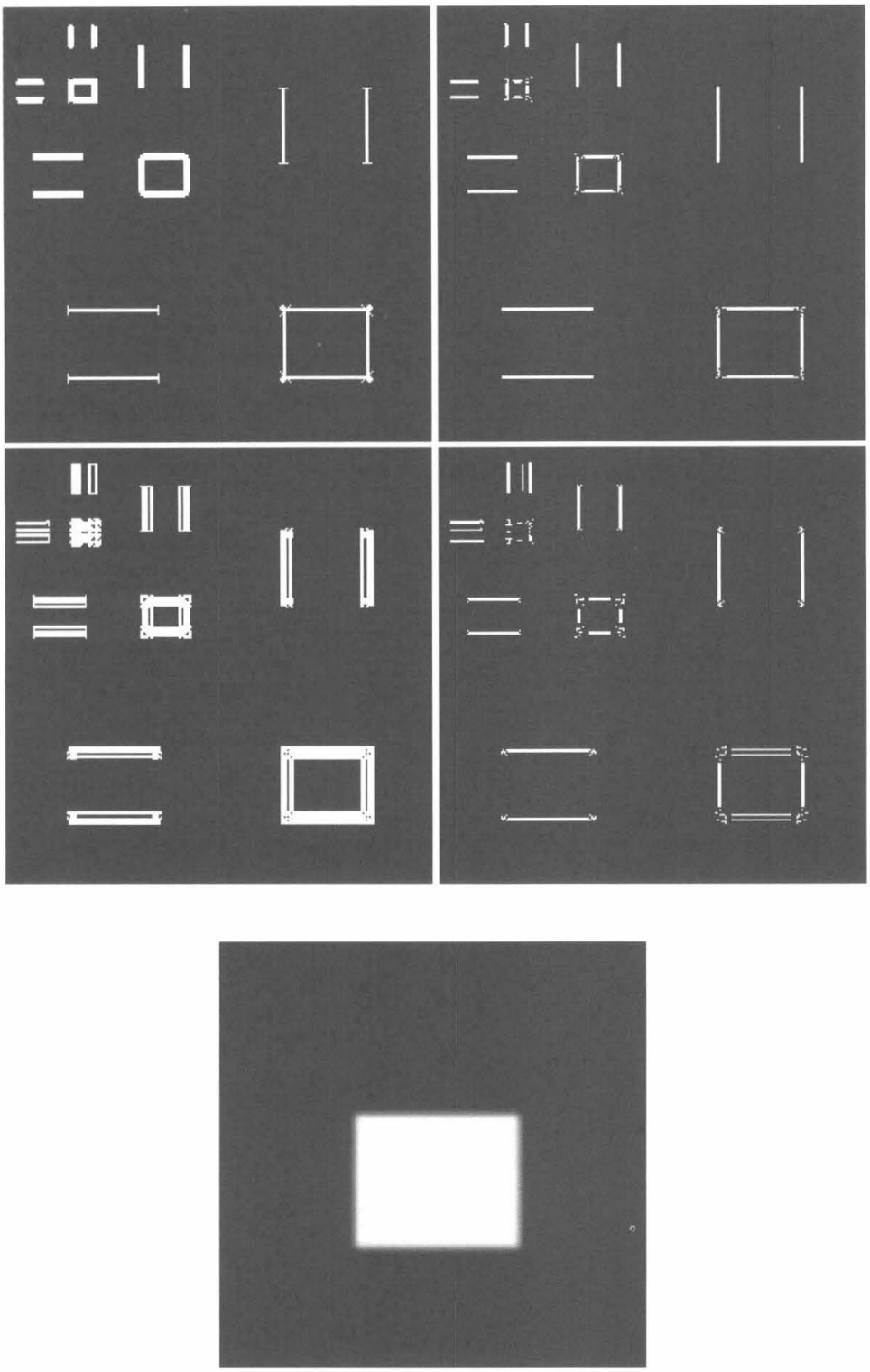

Fig. 3 Examples of zero-crossing maps. The bottom is a given image. The left and right are zero crossings before and after neighborhood processing using "Laplacian pyramid filters" (upper) and "spline variant filters" (middle) in three level wavelet decompositions, respectively. Notice the parent-child spatial coherence relation.

intensity that do not propagate to coarser scales can be removed for noise suppression.

3.2 *Adaptive Enhancement Algorithm*

The proposed adaptive enhancement scheme is shown in Fig. 5. On completion of the wavelet filtering and down-sampling to a desired decomposition level, the adaptive enhancement scheme can be applied to these decomposed subimages. There are three basic steps in the proposed enhancement algorithm: zero-crossing detection, zero-crossing tree establishment, and integrated adaptive enhancement. With zero-crossing detection, we are able to

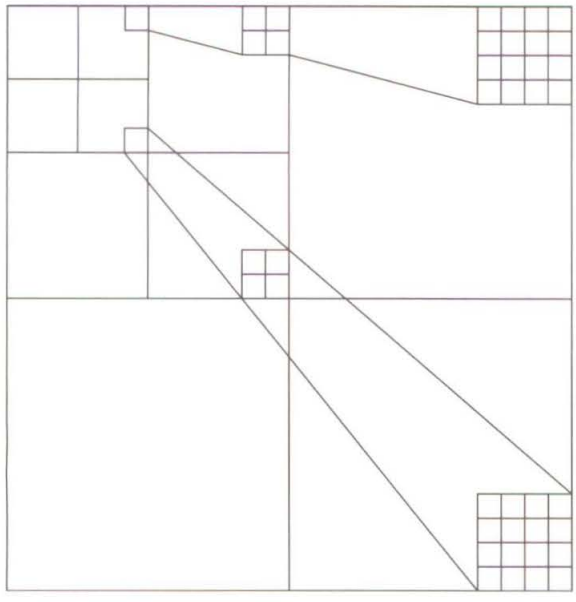

Fig. 4 Parent-child location relations.

locate the accurate position of the image features within each subimages. Since not all edges are considered useful features for mammographic image enhancement, we establish the zero-crossing tree according to the spatial coherence of image features. Only these edges within this zero-crossing tree are enhanced to ensure that the mammographic image features, not image noises, are indeed enhanced. Furthermore, to achieve an optimal visualization of the features governed by Weber's law, the baseband information is also incorporated into the enhancement algorithm.

As discussed, the zero crossings in subimages characterize the edge structure of the image. These edges correspond to potential microcalcifications and therefore must be enhanced. Among the zero crossings in the high-pass-filtered subimages, those with locally maximum variation rate of wavelet coefficients are important to represent the local edge features. To locate these zero crossing, we introduce neighborhood configurations for the algorithm to achieve its adaptivity to the local intensity variation. Three types of neighborhood configurations are used in this research, namely, a 1-D horizontal neighborhood, a 1-D vertical neighborhood, and a 2-D diagonal neighborhood, as shown in Fig. 6. These configurations correspond to the high-pass filters used in wavelet decomposition: a horizontal filter for HL subimage, a vertical filter for LH subimages, and a diagonal for HH subimage. With these neighborhood masks, zero crossings that pass through the local maximum variation rate test are assigned as "selected zero crossing" and are used in the next step of processing (also see Fig. 3).

The next step of processing aims to recognize the spatial coherence of the image features from the selected zero crossings to establish a zero-crossing tree. A selected zero crossing is considered part of the zero-crossing tree if it passes the parent-child location relationship test. That is, a selected zero crossing is attached to the zero-crossing tree if its parent is also a selected zero crossing and descends from the root of the zero-crossing tree. With this spatial coherence test, the zero crossings in the zero-crossing trees will include those image structure with parent-child location relationship rather than the noise, which would not have such a relationship due to its random nature. The established zero-crossing trees represent the evolution of edge structure from coarse resolution levels to fine resolution levels. In the case of adaptive enhancement of mammographic images, only these wavelet coefficients corresponding to zero crossings within the zero-crossing tree are scaled to achieve the desired enhancement results.

Once the zero-crossing tree is established, the information from baseband can be integrated with the enhancement in the high-pass-filtered subimages. In the case of global shift of baseband intensity value, if needed, an appropriate constant is added to every pixel in the baseband to increase the overall brightness so that subtle discrimination can be perceived after the shift. In the case of weighted enhancement of high-pass subimages, the weighting function is inversely proportional to the illumination levels in the corresponding neighborhood in baseband subimages. This operation enables radiologists to achieve a balanced brightness discrimination across the whole dynamic range of the display device.

If we denote $E^{a}_{m,n}$ and $E^{c}_{m,n}$ as the proposed operators for processing low-pass filtered (baseband) and high-pass filtered components, respectively, with the spatial position l and at level m, in 1-D case, the reconstruction of the enhanced image can be written as

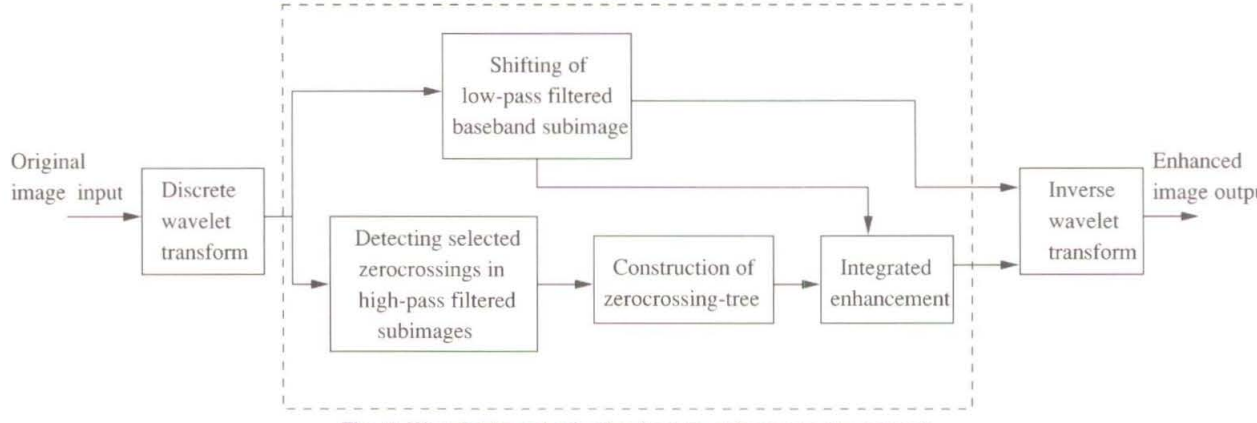

Fig. 5 Wavelet-based adaptive feature enhancement approach.

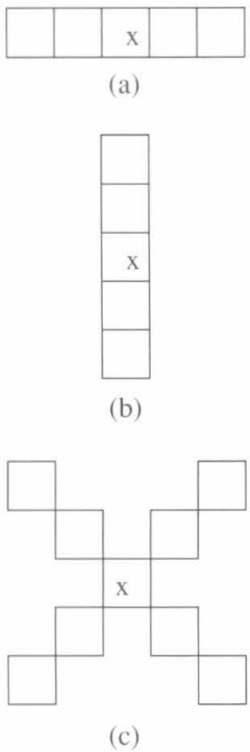

Fig. 6 Typical neighborhoods for (a) HL subimage processing, (b) LH subimage processing, and (c) HH subimage processing; *x* is the selected zero crossing if it has maximum variation rate in the neighborhood.

$$\begin{aligned}\bar{a}_{m-1,l}(f) &= \sum_n \{\bar{h}_{2n-l}E^a_{m,n}[a_{m,n}(f)] \\ &\quad + \bar{g}_{2n-l}E^c_{m,n}[c_{m,n}(f)]\} \\ &= a_{m-1,l}(f) \\ &\quad + \sum_n [\bar{h}_{2n-l}\{E^a_{m,n}[a_{m,n}(f)] - a_{m,n}(f)\} \\ &\quad + \bar{g}_{2n-l}\{E^c_{m,n}[c_{m,n}(f)] - c_{m,n}(f)\}), \end{aligned} \tag{5}$$

which indicates that the enhanced image equals the original image plus a summation term that includes component differences in baseband subimage and high-pass-filtered subimage. If no processing in baseband, the first term in the summation will be zero. For baseband enhancement, the shift can be easily defined as

$$E^a_{m,n}[a_{m,n}(f)] = a_{m,n}(f) + b, \tag{6}$$

where b is a shift constant. Such an overall shift can preserve the relative gray-level distribution of the original image. For the weighted scaling used in the enhancement of high-pass-filtered subimages, the weighting function can be written as

$$P(x_{m,n}) \propto \left(\alpha \sum_{s \in N_n} x_{m,s} + \beta \right)^{-1}, \tag{7}$$

where α and β are constant parameters, and N_n represents a defined neighborhood for position n. With such weighting function the enhancement operator can be expressed as

$$E^c_{m,n}[c_{m,n}(f)] = P[a_{m,n}(f)]c_{m,n}(f) \tag{8}$$

if $c_{m,n}(f)$ is in the zero-crossing tree.

4 Experimental Results

For the convenience of display, the original images from Nijmegen's database have been clipped with the region of interest and subsampled, and resulted in 512×512 images. In this experiment, "Laplacian pyramid filters (5/7)" (Ref. 25) are selected to compute discrete wavelet transform because the filters are nearly orthonormal filters with moderate lengths. The width or height of the neighborhood mask was chosen to be the same as the length of wavelet filters, since this has been shown to produce empirically better results. Prior information about microcalcification details in mammographic image is used to guide the choice of desired decomposition levels. Some typical experimental results for the images from the database are shown in Figs. 7 to 10. Note that the microcalcifications appeared in each image. The upper left figures are original images and the upper right figures are images enhanced with the proposed approach, the lower left and the lower right figures are images using unsharp masking and high-pass filtering.

It is evident from Figs. 7 to 10 that the shifting processing for baseband subimage improves global visualization over the original images. Together with the weighted scaling using the illumination level of the baseband subimage, the proposed enhancement scheme is able to make some unseen or barely seen features visible. The zero-crossing-tree-based processing enables us to enhance those structures in which we are interested while suppressing noise.

5 Summary

We have presented a novel and computationally efficient approach to adaptive mammographic image feature enhancement and noise suppression using wavelet-based multiresolution analysis. We integrate information of the tree-structured zero crossing of wavelet coefficients and information of the low-pass-filtered subimage to achieve robust and optimal enhancement. The spatiofrequency localization property of the wavelet transform is exploited based on the spatial coherence of the image and the principle of the human psychovisual mechanism. Preliminary results show that the proposed approach is able to adaptively enhance local edge features, suppress noise, and improve global visualization of mammographic image features. This wavelet-based multiresolution analysis is therefore promising for computerized mass screening of mammograms.

This multiresolution analysis scheme can be extended to feature extraction applications to extract microcalcifications from mammographic images. By incorporating the shape and size knowledge of the microcalcification, we will be able to develop a robust feature extraction algorithm suitable for computerized mass screening of mammograms as well as CAD with real-time implementation potential.

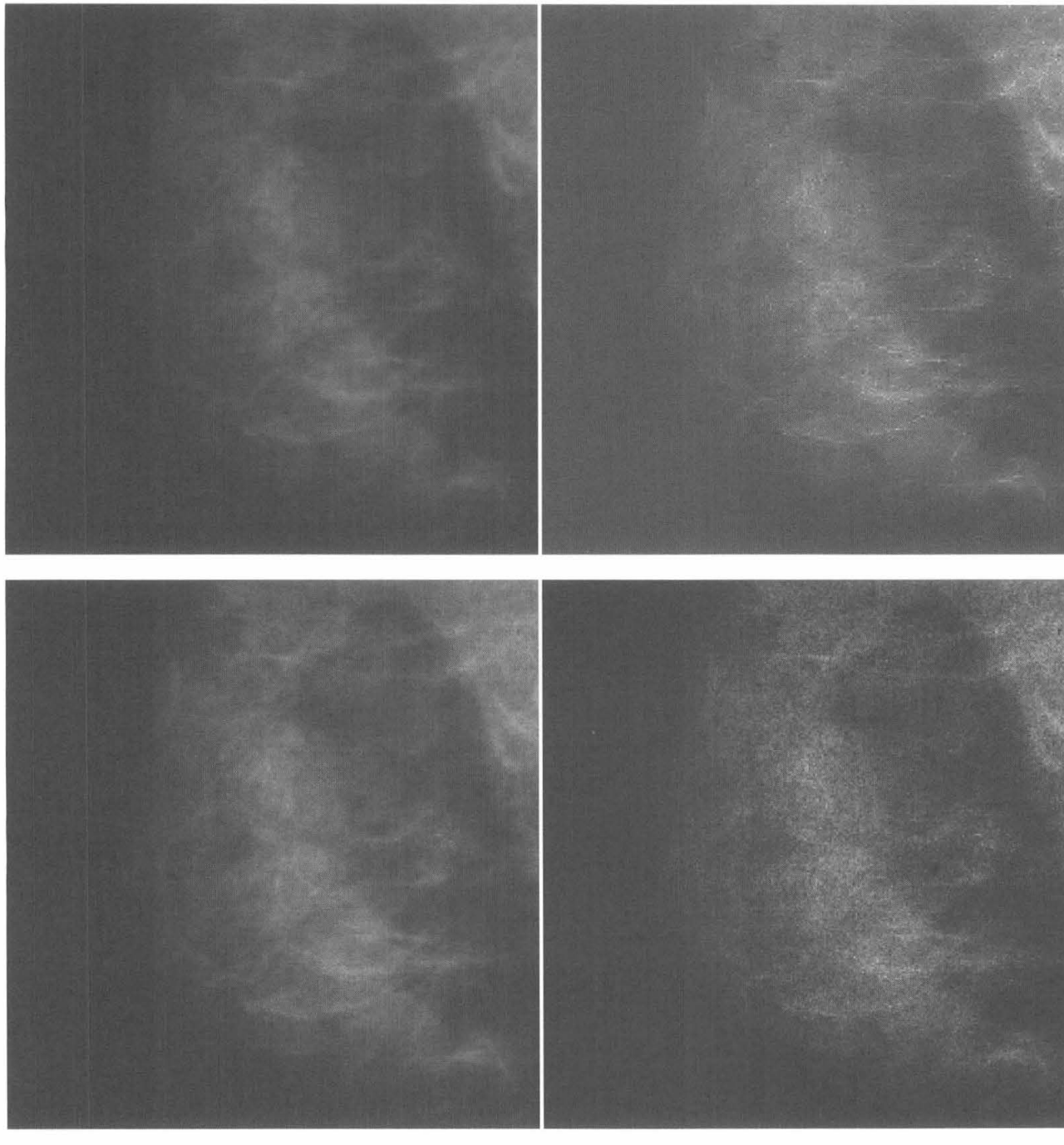

Fig. 7 Experimental results: the upper left is the original image and the upper right is the image enhanced with the proposed approach, the lower left and the lower right are images using unsharp masking and high-pass filtering, respectively. Microcalcifications appear at the location (421,245) with radius of 48.

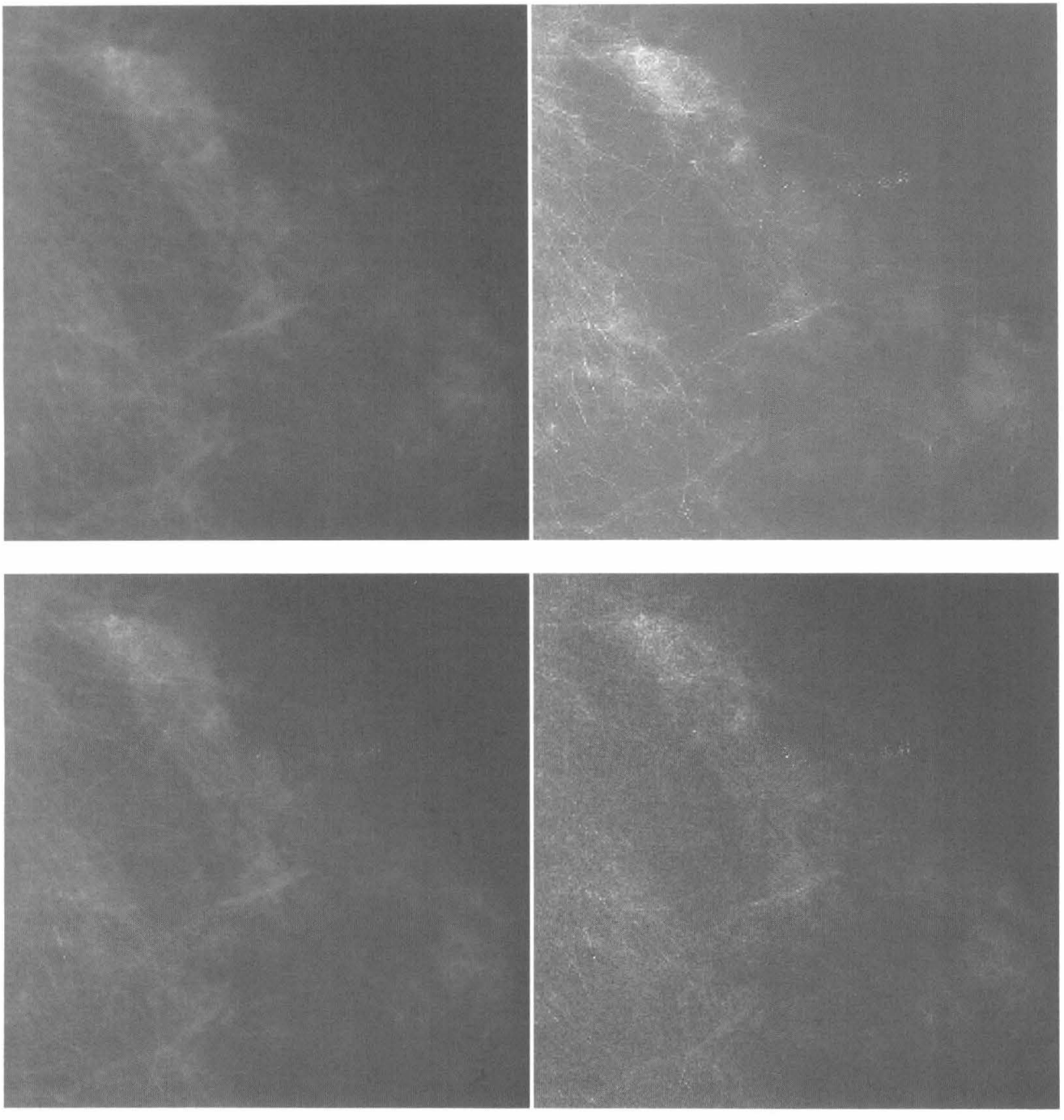

Fig. 8 Experimental results: the upper left is the original image and the upper right is the image enhanced with the proposed approach, the lower left and the lower right are images using unsharp masking and high-pass filtering, respectively. Microcalcifications appear at the location (298,165) with radius of 105.

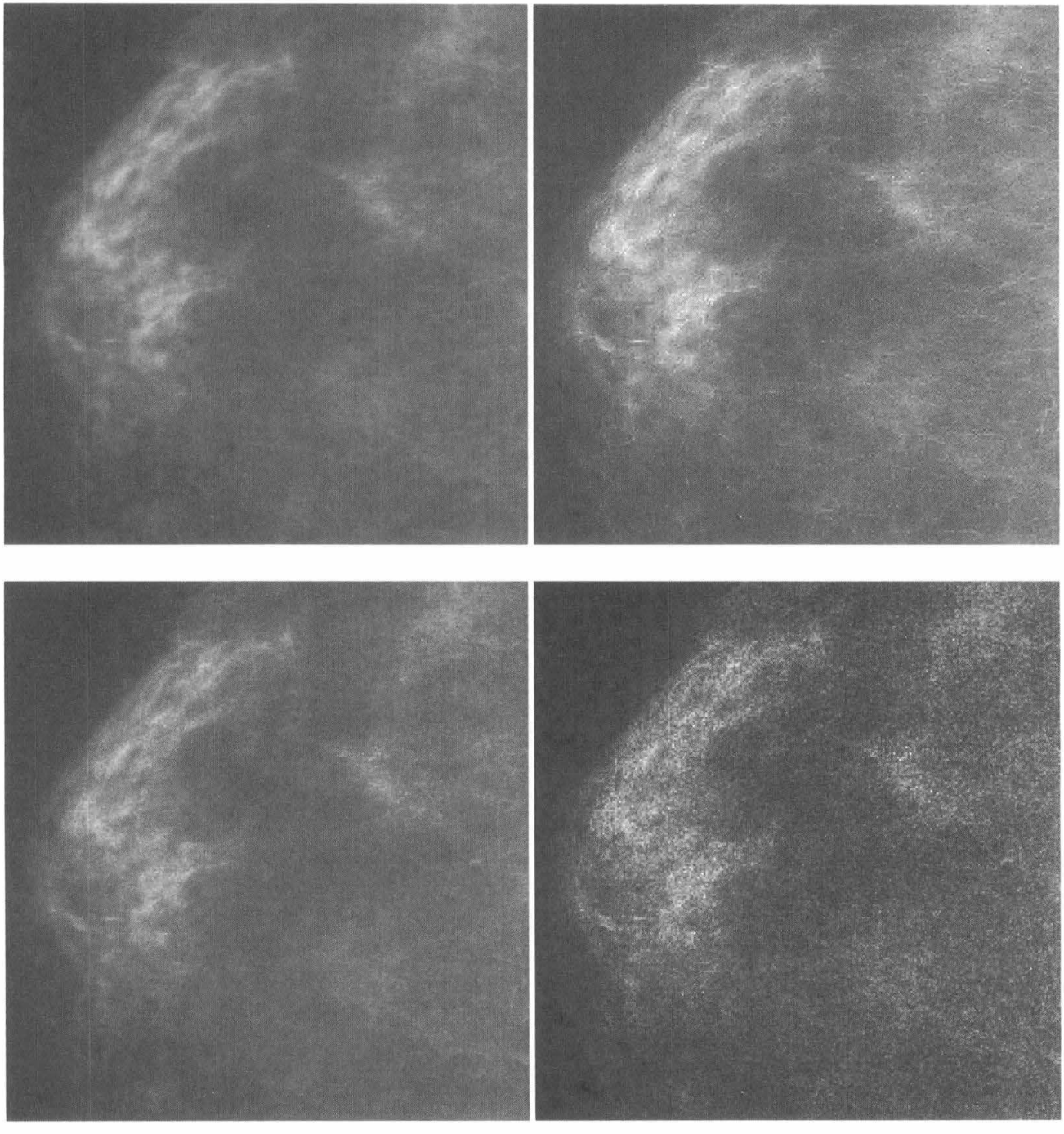

Fig. 9 Experimental results: the upper left is the original image and the upper right is the image enhanced with the proposed approach, the lower left and the lower right are images using unsharp masking and high-pass filtering, respectively. Microcalcifications appear at the location (360,176) with radius of 79.

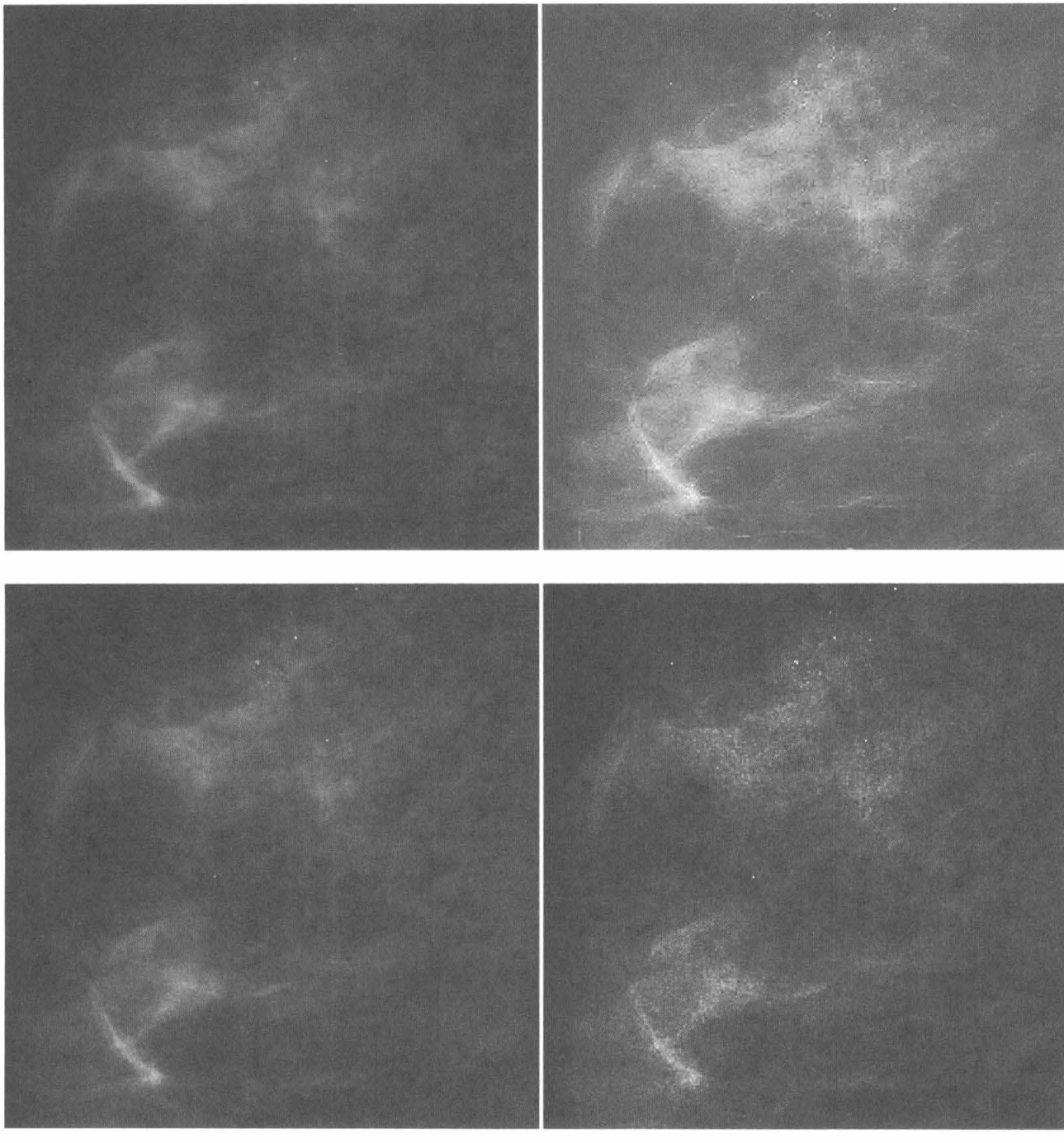

Fig. 10 Experimental results: the upper left is the original image and the upper right is the image enhanced with the proposed approach, the lower left and the lower right are images using unsharp masking and high-pass filtering, respectively. Microcalcifications appear at the location (274,30) with radius of 99.

Acknowledgments

This research is supported by American Cancer Society Grant ACS-IRG-18-38, National Science Foundation Grant EEC-92-09615, and a New York State Science & Tech. Foundation Grant to the Center for Electronic Imaging. The images were provided by the courtesy of the National Expert and Training Centre for Breast Cancer Screening and the Department of Radiology at the University of Nijmegen, the Netherlands. The authors would thank Dr. Arvin Robinson at the Department of Radiology, University of Rochester, for his clinical evaluation of the mammographic images.

References

1. A. Tucker and P. Last, "Cancer screening and research," *Physicians Bull.* **39**, 190–191 (1988).
2. H. A. Frazer, "Computerized diagnosis comes to mammography," *J. of Diagn. Imag.* **13**(6), 91–95 (June 1991).
3. L. Tabar and P. B. Dean, "Basic principles of mammographic diagnosis," *Diagn. Imag. Clin. Med.* **54**, 146–157 (1985).
4. A. G. Gale, S. M. Astley, D. R. Dance, and A. Y. Cairns, Eds., *Digital Mammography*, Elsevier Science, Amsterdam (1994).
5. A. P. Dhawan and E. L. Royer, "Mammographic feature enhancement by computerized image processing," *Comput. Meth. Progr. Biomed.* **27**(1), 23–35 (1988).
6. D. Brzakovic, X. M. Luo, and P. Brzakovic, "An approach to automated detection of tumors in mammograms," *IEEE Trans. Med. Imag.* **9**, 232–241 (Sep. 1990).
7. H. P. Chan, K. Doi, S. Galhotra, C. J. Vyborny, and H. M. and P. M. Jokich, "Image analysis and computer-aided diagnosis in digital radiography, automated detection of microcalcifications in mammography," *Med. Phys.* **14**, 538–548 (July 1987).
8. H. P. Chan, K. Doi, C. J. Vyborny, K. L. Lam, and R. A. Schmidt, "Computer-aided detection of microcalcifications in mammograms," *Invest. Radiol.* **23**, 664–671 (Sep. 1988).
9. S. Lai, X. Li, and W. F. Bischof, "On techniques for detecting circumscribed masses in mammograms," *IEEE Trans. Med. Imag.* **8**, 377–386 (Dec. 1989).
10. R. Gordon and R. M. Rabgayyan, "Feature enhancement of film mammograms using fixed and adaptive neighborhoods," *Appl. Opt.* **23**, 560–564 (Feb. 1984).
11. A. Giles, A. R. Cowen, and G. J. S. Parkin, "A clinical workstation for digital mammography," *Proc. SPIE* **1905**, 806–817 (1993).
12. A. F. Laine, S. Schuler, J. Fan, and W. Huda, "Mammographic feature enhancement by multiscale analysis," *IEEE Trans. Med. Imag.* **13**, 725–740 (Dec. 1994).
13. W. B. Richardson, "Nonlinear filtering and multiscale texture discrimination for mammograms," in *Mathematical Methods in Medical Imaging, Proc. SPIE* **1768**, 293–305 (July 1992).
14. A. Laine and S. Song, "Wavelet processing techniques for digital mammography," in *Visualization in Biomedical Computing, Proc. SPIE* **1808**, 610–624 (Oct. 1992).
15. R. N. Strickland and H. I. Hahn, "Wavelet transform matched filters for the detection and classification of microcalcifications in mammography," in *Proc. IEEE Int. Conf. Image Processing*, Vol. I, pp. 422–425, Washington, DC (Oct. 1995).
16. W. Qian and L. P. Clarke, "Adaptive multistage nonlinear filtering and wavelet for medical image enhancement," in *Proc. R. IEEE Int. Conf. Image Processing*, vol. II, pp. 711–715, Austin, TX (Nov. 1994).
17. S. Mallat and S. Zhong, "Characterization of signal from multiscale edges," *IEEE Trans. Pattern Anal. Mach. Intell.* **14**, 710–732 (July 1992).
18. S. Mallat, "Zero-crossing of a wavelet transform," *IEEE Trans. Inf. Theory* **37**, 1019–1033 (July 1991).
19. J. Canny, "A computational approach to edge detection," *IEEE Trans. Pattern Anal. Mach. Intell.* **8**, 679–698 (Nov. 1986).
20. D. Marr and E. Hildreth, "Theory of edge detection," *Proc. R. Soc. London* **207**, 187–217 (1980).
21. I. Daubechies, "The wavelet transform, time-frequency localization and signal analysis," *IEEE Trans. Inf. Theory* **36**, 961–1005 (1990).
22. S. G. Mallat, "A theory for multiresolution signal decomposition: the wavelet representation," *IEEE Trans. Pattern Anal. Mach. Intell.* **11**, 674–693 (July 1989).
23. R. C. Gonzalez and R. E. Woods, *Digital Image Processing*, Addison-Wesley, Reading, MA (1992).
24. A. Cohen, I. Daubechies, and J. C. Feauveau, "Biorthogonal bases of compactly supported wavelets," AT&T Bell Lab., Technical Report TM 11217-900529-07 (1990).
25. M. Antonini, M. Barlaud, P. Mathieu, and I. Daubechies, "Image coding using wavelet transform," *IEEE Trans. Image Process.* **1**, 205–220 (Apr. 1992).
26. S. Mallat and W. L. Hwang, "Singularity detection and processing with wavelet," *IEEE Trans. Inf. Theory* **38**, 617–643 (Mar. 1992).

Lulin Chen received a BS in electrical engineering from the University of Science and Technology of China (USTC) in 1982, an MS in electrical engineering from East China Normal University in 1985, and a PhD in electrical-optical engineering from Shanghai Institute of Technical Physics, Chinese Academy of Sciences, in 1992 and joined the faculty there as an associate researcher. He was a doctoral researcher at the Institute of Industrial Sciences at University of Tokyo, Japan, from 1993 to 1994. Since 1995 he has been with Department of Electrical Engineering at University of Rochester. His research interests include image/video processing, data compression, pattern recognition, and neural networks.

Chang W. Chen received his BS degree in electrical engineering from the University of Science and Technology of China in 1983, his MSEE degree from the University of Southern California, Los Angeles in 1986, and his PhD degree in electrical engineering from the University of Illinois at Urbana-Champaign in 1992. From August 1992 to September 1996, he was on the faculty of the Department of Electrical Engineering, University of Rochester. Since September 1996, he has been an Assistant Professor in the Department of Electrical Engineering at the University of Missouri-Columbia. He received the Best Paper Award at the 1994 SPIE Conference on Visual Communication and Image Processing, and the Whitaker Foundation Biomedical Engineering Research Award in 1996. His current research interests include image and video coding, image communication, biomedical image understanding, computer vision, and scientific visualization. He is an Associate Editor for *IEEE Trans. Circuits and Systems for Video Technology*, and a member of IEEE, SPIE, and Tau Beta Pi.

Kevin J. Parker received the BS degree in engineering science, summa cum laude, from the State University of New York at Buffalo in 1976. His graduate work in electrical engineering was completed at the Massachusetts Institute of Technology, with MS and PhD degrees received in 1978 and 1981. From 1981 to 1985 he was an assistant professor of electrical engineering at the University of Rochester; currently he holds the title of professor of electrical engineering and radiology. Dr. Parker has received awards from the National Institute of Medical Sciences (1979), the Lilly Teaching Endowment (1982), the IBM Supercomputing Competition (1989), and the World Federation of Ultrasound in Medicine and Biology (1991). He is a member of the IEEE Sonics and Ultrasonics Symposium Technical Committee and serves as reviewer and consultant for a number of journals and institutions. He is also a fellow of the IEEE and is on the board of governors of the American Institute of Ultrasound in Medicine. Dr. Parker's research interests are in medical imaging, linear and nonlinear acoustics, and digital halftoning.